Pergamon

Int. J. Heat Mass Transfer. Vol. 41, Nos 6–7, pp. 871–879, 1998

Printed in Great Britain
0017-9310/98 $19.00+0.00

PII: S0017-9310(97)00175-0

An asymptotic model of work roll heat transfer in strip rolling

R. E. JOHNSON and R. G. KEANINI†

Department of Mechanical Engineering and Engineering Science, University of North Carolina at Charlotte, Charlotte, NC 28223, U.S.A.

(*Received* 20 *November* 1996 *and in final form* 4 *June* 1997)

Abstract—An asymptotic model of work roll heat transfer is developed using a multiple time scale approach. The model is appropriate under typical high Peclet number rolling conditions and provides a unified framework for relating previous roll heat transfer models. The solution consists of a fast time scale thermal boundary layer near the roll surface, along with a slow time scale core heat transfer problem. Several features of the model are illustrated. First, boundary layer behavior is examined under steady and dynamic conditions. Here, the decay rate for boundary layer transients is determined and theoretical steady-state temperature distributions are compared against previously reported experimental data. Heat transfer within the core is then considered under relatively general surface heating conditions. In the special case where the surface heat flux is constant, core temperatures are shown to increase linearly with time. In the last illustration, the model is used to obtain inverse estimates of circumferentially varying roll surface heat flux and temperature distributions. In this case, comparisons are made with the finite difference-based inverse estimates recently reported by Huang *et al.*, *International Journal of Heat and Mass Transfer*, 1995, **38**, 1019–1031. © 1997 Elsevier Science Ltd.

INTRODUCTION

A number of models describing work roll heat transfer have appeared in the last 30 years [1–9], beginning with Peck's work in 1954 [1]. Most models assume a cyclic steady-state [2–8], and under typical high Peclet number conditions, indicate the presence of a near surface thermal boundary layer. Although true steady-state conditions can only appear following long rolling periods, i.e. time periods on the order of $\hat{R}^2/\alpha_0$ (where $\hat{R}$ is the roll radius and α_0 the roll thermal diffusivity), or in rare cases where roll cooling exactly matches roll heating, recent experimental measurements [10, 11] show that nominally steady conditions exist within the near surface region, at least over time spans on the order of several (~ 10) roll periods.

Upsets in the steady-state thermal boundary layer accompany changes in roll heating conditions, e.g. when a new coil contacts the roll. An important question which bears, for example, on process control or inverse estimation, concerns the amount of time required for a new steady state to set in. Guo's [9] work peripherally addresses this question by circumferentially averaging the surface flux distribution. While this approach allows examination of unsteady effects, it cannot provide detailed information on the boundary layer adjustment time. Indeed, it appears that this question has not been rigorously addressed.

Due to the typical mismatch between roll heating and cooling, the roll core can heat up and cool down in time. While boundary layer heat transfer occurs over time scales on the order of $\hat{\Omega}^{-1}$ (where $\hat{\Omega}$ is the roll rotation rate), core heat transfer occurs over much slower time scales determined by process heating and cooling variations. Due to the disparate difference between these time scales, it is extremely difficult to develop models which allow efficient calculation of heat transfer within both the boundary layer and within the core. This difficulty is reflected in the fact that present models either assume cyclically steady conditions [2–8] or incorporate circumferential averaging [9].

This article develops a multiple-time scale asymptotic model of work roll heat transfer. The formulation provides a unified framework for relating previous boundary layer and core heat transfer models and provides a general basis for developing future models. We illustrate the model by: (i) examining transient and steady heat transfer within the near-surface thermal boundary layer; (ii) determining core heat transfer under general surface heating conditions; and (iii) applying the model to estimate circumferential surface heat flux and temperature distributions on a work roll. The first and last illustrations allow comparisons with recently reported experimental measurements.

ASYMPTOTIC MODEL OF WORK ROLL HEAT TRANSFER

A simple schematic of the rolling process is shown in Fig. 1. A work roll of radius $\hat{R}$ rotates with angular

† Author to whom correspondence should be addressed.

NOMENCLATURE

A	roll aspect ratio
c_p; c_{p1}, c_{p2}	specific heat; dimensionless coefficients in definition of c_p
k; k_1, k_2	thermal conductivity; dimensionless coefficients in definition of k
N	number of temperature measurements used in inverse procedure
q	heat flux
r	radial coordinate
R	roll radius
S	augmented least square function given in eqn (10)
t	time
T	temperature.

Greek symbols

α_0	reference thermal diffusivity
$\gamma(T)$	dimensionless function in eqn (1), $(c_{p1}+c_{p2})^{-1}$
δ	characteristic distance
ε	inverse Peclet number
η	stretched radial distance in boundary layer
θ	angular coordinate
κ	uniform random deviate
τ	time scale
Ω	roll rotation rate.

Subscript

0	reference value; leading order.

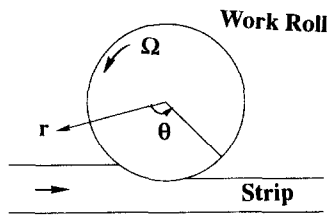

Fig. 1. Schematic of the rolling process and the coordinate system (adapted from [10]).

velocity $\hat{\Omega}$ and has a constant initial temperature $\hat{T}_i$. The roll width (not shown) is $\hat{L}$ while the workpiece width, $\hat{L}_w$, can, in general, vary from coil to coil. Within the work roll, the dimensionless conduction equation assumes the form

$$\frac{\partial T}{\partial t}+\frac{\partial T}{\partial \theta}=\frac{1}{Pe}\gamma(T)\nabla_1\cdot[k(T)\nabla_1 T] \qquad (1)$$

where $Pe=\hat{\rho}_0\hat{c}_{p0}\hat{\Omega}\hat{R}^2/k_0$ is the Peclet number, $T=(\hat{T}-\hat{T}_i)/\Delta\hat{T}_s$ is the dimensionless temperature, $\Delta\hat{T}_s=\hat{q}_s\hat{R}/\hat{k}_0$ is the characteristic temperature scale, $\hat{q}_s$ is the characteristic applied heat flux, $\nabla_1=\hat{e}_r\,\partial/\partial r+\hat{e}_\theta\,1/r\,\partial/\partial\theta+\hat{e}_z A\,\partial/\partial z$, is the dimensionless divergence operator, $A=\hat{R}/\hat{L}$, is the roll aspect ratio, $r=\hat{r}/\hat{R}$, $z=\hat{z}/\hat{L}$, and $t=\hat{\Omega}\hat{t}$. The functions $\gamma(T)=(c_{p1}+c_{p2}T)^{-1}$ and $k(T)=k_1+k_2T$ arise from our definitions of density, specific heat and thermal conductivity: $\hat{\rho}=\hat{\rho}_0$, $\hat{c}_p(T)=\hat{c}_{p0}(c_{p1}+c_{p2}T)$, and $\hat{k}(T)=\hat{k}_0(k_1+k_2T)$. Here, $\hat{\rho}_0$, $\hat{c}_{p0}$ and $\hat{k}_0$ are reference magnitudes and the dimensionless constants k_1, k_2, c_{p1} and c_{p2} are determined from two-term expressions for $\hat{c}_p(\hat{T})$ and $\hat{k}(\hat{T})$ [12]. Throughout, dimensional quantities are denoted with a caret.

In the present study, the aspect ratio A is small, i.e. the roll is long compared to its radius. Thus, axial temperature variations are small relative to those in the radial and azimuthal directions. This is apparent in eqn (1) where A multiplies $\partial/\partial z$ in the operator ∇_1. Consequently, the solutions obtained will apply over most of the roll's length, where axial conduction is weak, but will not hold near the roll's end, $z=1$, where a boundary layer must exist in order to accommodate prescribed heat flux boundary conditions. Similarly, solutions may break down near workpiece edges due to locally large axial temperature gradients. Neither of these regions are considered in this paper.

Under typical high speed rolling conditions with steel work rolls, $\Omega^{-1}\sim 0.05$ s, $\hat{R}\sim 0.3$ m, and $\hat{k}_0/\hat{\rho}_0c_{p0}=10^{-5}\,\mathrm{m^2\,s^{-1}}$. Consequently, the Peclet number is large, i.e. the rotation rate is fast compared to the diffusion time scale within the roll. Thus, under typical conditions where heat is added and removed over various portions of the roll circumference, a thin thermal boundary layer is present at the roll surface, $r=1$. As mentioned, Huang *et al.* [10] provide experimental evidence showing that the azimuthally varying surface flux distribution remains nominally time-invariant, at least over time spans on the order of several roll rotation periods. In contrast, experimental evidence [13] indicates that circumferentially averaged flux distributions vary on a slow time scale determined by changing operating conditions. Consequently, the problem is one of multiple time scales: a fast time $t=\hat{\Omega}\hat{t}$ determined by the roll rotation rate, and a slow, process-related time scale.

To tackle this problem, the heat flux at the roll surface is modeled by a prescribed function that varies over a slow time scale. This leads to a dimensionless boundary condition on the roll surface $r=1$ given by

$$k(T)\frac{\partial T}{\partial r}=\bar{q}(z,\tilde{t})+q'(z,\theta,\tilde{t}) \qquad (2)$$

where $\tilde{t}$ is the slow time scale defined by $\tilde{t}=Pe^{-1}t$, and where q' has zero circumferential mean

$$\int_0^{2\pi} q' \, d\theta = 0. \tag{3}$$

Typically, at the end of the roll, $z = 1$, there is negligible heat flux and an appropriate boundary condition is

$$k(T)\frac{\partial T}{\partial z} = 0. \tag{4}$$

This condition appears to hold during hot soaking (when the roll is preheated prior to rolling) and when strip widths are somewhat less than the roll width [13]. Conditions at $r = 0$ and $z = 0$ are given below. Note, if a significant heat flux exists at the roll ends, eqn (4) can be modified.

To accommodate the boundary condition (2), the solution to (1) is divided into two terms,

$$T = \bar{T}(r, z, \tilde{t}) + T'(r, \theta, z, t, \tilde{t}). \tag{5}$$

The first term evolves on the slow time scale, t, and accounts for roll heating by the circumferentially averaged surface heat flux $\bar{q}$. The second term T' is introduced in order to accommodate the azimuthal heat flux variation. This term must: (i) allow for transient responses that occur on the fast time scale; (ii) accommodate possible slow time scale evolution; and (iii) provide the steady boundary layer temperature distribution under steady-state conditions. Substituting (5) into (1) we obtain

$$\frac{\partial T'}{\partial t} + \frac{\partial T'}{\partial \theta} + \frac{1}{Pe}\left(\frac{\partial \bar{T}}{\partial \tilde{t}} + \frac{\partial T'}{\partial \tilde{t}}\right) = \frac{\gamma(T)}{Pe} \times (\nabla_1 \cdot (k(T)\nabla_1 \bar{T}) + \nabla_1 \cdot (kT)\nabla_1 T')). \tag{6}$$

Due to the large Peclet number, we have a hierarchy of problems to consider. At $O(1)$,

$$\frac{\partial T'}{\partial t} + \frac{\partial T'}{\partial \theta} = 0. \tag{7}$$

Using the initial condition $T' = 0$, and writing (7) in characteristic form shows that the solution is

$$T' \equiv 0. \tag{8}$$

However, since this does not satisfy the surface boundary condition on $r = 1$

$$k(T)\frac{\partial T'}{\partial r} = q'(\theta, z, \tilde{t}) \tag{9}$$

a thermal boundary layer solution is required near $r = 1$. Introducing the boundary layer coordinate $\eta = \sqrt{Pe}(1-r)$ and considering a solution to eqn (6) having the form $T' = T'[\eta, \theta, z, t, \tilde{t}]$. we obtain the thermal boundary layer problem

$$\frac{\partial T'}{\partial t} + \frac{\partial T'}{\partial \theta} = \gamma(T)\frac{\partial}{\partial \eta}\left(\frac{k(T)\,\partial T'}{\partial \eta}\right) \tag{10}$$

$$T' = 0 \quad \text{at } t = 0 \tag{11}$$

$$k(T)\frac{\partial T'}{\partial \eta} = -\frac{1}{\sqrt{Pe}} q'(\theta, z, \tilde{t}) \tag{12}$$

with matching condition

$$T' \to 0 \quad \text{as } \eta \to \infty. \tag{13}$$

Since $A/Pe \ll 1$ in most practical problems, the axial conduction term has been neglected in obtaining (10). Thus, z functions only as a parameter in (9) and (12), i.e. the solution to T' only depends on the local (though typically axially-varying) flux distribution. As such (and as mentioned), the solution is valid over most of the roll's length, but fails in a small neighborhood of the roll's end, $z = 1$. An additional boundary layer would be required in order to complete the solution in this region. Note that the axial flux variation imposed in (12) is compatible with neglect of axial conduction, provided that this variation is not severe.

We note that under steady-state conditions and for constant thermophysical properties, the boundary layer problem in (10)–(13) simplifies to the problem considered by Yuen [8] and Tseng [6, 10]. Although Patula [2] and Yuen [3] did not formulate their models in terms of the thermal boundary layer, their solutions nevertheless approach the boundary layer solution as Pe becomes large [2, 3]. (Refer to Table 1.)

At the next order, $O(Pe^{-1})$, we have

$$\frac{\partial \bar{T}}{\partial \tilde{t}} + \frac{\partial T'}{\partial \tilde{t}} = \gamma(T)[\nabla_1 \cdot (k(T)\nabla_1 \bar{T}) + \nabla_1 \cdot (k(T)\nabla_1 T')] \tag{14}$$

which simplifies to

$$\frac{\partial \bar{T}}{\partial \tilde{t}} = \gamma(T)\nabla_1 \cdot [(k(T)\nabla_1 \bar{T})] \tag{15}$$

throughout the roll. Associated boundary and initial conditions are

$$\bar{T} = 0 \quad \tilde{t} = 0 \tag{16a}$$

$$k(T)\frac{\partial \bar{T}}{\partial r} = \bar{q}(z, \tilde{t}) \quad r = 1 \tag{16a}$$

$$\frac{\partial \bar{T}}{\partial r} = 0 \quad r = 0 \tag{16b}$$

$$\frac{\partial \bar{T}}{\partial z} = 0 \quad z = 1 \tag{16c}$$

$$\frac{\partial \bar{T}}{\partial z} = 0 \quad z = 0. \tag{16d}$$

[Refer to eqn (8) and note that (16b) and (16d) are assumed symmetry conditions.]

COMPARISON WITH PREVIOUS MODELS

A representative summary of recent work roll heat transfer models is given in Table 1. The table indicates

Table 1. Representative roll heat transfer models

Ref.	Equivalent governing equation	Assumptions–simplifications	Thermo-physical properties	Solution method	Comments
[2]	(10)	steady	constant	analytical	1, 2, 6
[3]	(10)	steady	constant	analytical	1, 2, 3, 6
[4]	(10)	steady	constant	numerical	1, 2, 6
[5]	(10)	steady	constant	analytical and numerical	2, 3, 4, 6
[6]	(10)	steady	constant	analytical	6
[7]	(10)	steady	constant	analytical	4, 5, 6, 7
[8]	(10)	steady	constant	analytical	2, 4, 6, 7
[9]	(15)	circumferentially avg'd. gov. eqn.	constant	analytical	2, 6, 8
[10]	(10)	—	constant	inverse-numerical	1, 9
[11]	(10)	—	constant	inverse-numerical	1, 9, 10
[13]	(15)	circumferentially avg'd gov. eqn.	constant	inverse-numerical	8, 11

1. Although the second derivative in the azimuthal direction is included, this term becomes negligible at high Pe. Axial temperature variations neglected.
2. Solutions based on specified flux distributions.
3. Effects of strip scale layer incorporated.
4. Treated boundary layer problem similar to (10).
5. Focused on heat transfer in the roll bite.
6. Experimental validation not performed due to lack of data.
7. Based on two-dimensional semi-infinite domain approximation.
8. Models core heat transfer over long time periods.
9. Used to obtain inverse-based estimate of azimuthal flux distribution.
10. Employed Lagrangian approach.
11. Used to obtain inverse-based estimate of time- and axially-dependent flux distributions over a period of approximately 3 h.

the relationship between previous models and the present model and includes direct models used in recent inverse calculations. While all listed models neglect thermophysical property variations, recent surface temperature measurements reported by Tseng *et al.* [11] and Huang *et al.* [10] show that roll surface temperatures can vary by approximately 400°C during each rotation. Thus, applications demanding high accuracy should incorporate temperature dependent thermophysical properties. Suitable solution methods can be adapted from those given in Refs [14] and [15].

As is also shown in Table 1, the problem in (15)–(16d) is equivalent to the problem recently solved by Guo [9]. As mentioned, this solution, obtained using Laplace transforms and spatial and temporal superposition, removes the azimuthal dependence by circumferentially averaging the flux distribution at $r = 1$. The model accommodates time-dependent (circumferentially-averaged), axially-varying roll surface flux distributions and can be used to simulate, e.g. multi-coil rolling and rolling of variable width strip [9]. Due to the length of his solution, the interested reader is referred to Ref. [9]. We also note that the problem defined in (15)–(16d) was recently used to obtain an inverse-based estimate of axially and temporally-varying work roll flux distributions [13]. The estimate was based on spatially discrete, embedded temperature measurements and was obtained using a finite difference-conjugate gradient approach.

MODEL ILLUSTRATION I: BOUNDARY LAYER HEAT TRANSFER

Dynamic boundary layer

In all illustrative examples, we neglect thermophysical property variations and obtain closed form solutions. The solutions are thus appropriate in cases where property variations are negligible or when high accuracy is not needed. Under these circumstances, $\gamma(T) = k(T) = 1$. In addition, we make the realistic assumption that the heat flux distribution q' does not vary on the slow time scale [10]. Based on these simplifications, we write eqn (10) in characteristic form

$$\frac{dT'}{dt} = \frac{\partial^2 T'}{\partial \eta^2} \tag{17}$$

$$\frac{d\theta}{dt} = 1 \rightarrow \theta - \theta_0 = t \tag{18}$$

where θ_0 is the initial position of a point in the roll.

A series solution useful for studying the dynamic behavior of T' can be determined by expanding q' in a Fourier series

$$\frac{\partial T'}{\partial \eta} = -\frac{1}{\sqrt{Pe}} q'(\theta, z) = -\frac{1}{\sqrt{Pe}} \sum_{n=0}^{\infty} a_n(z) \cos n\theta \tag{19}$$

$$= -\frac{1}{\sqrt{Pe}}\sum_{n=0}^{\infty} a_n(z)[\cos n\theta_0 \cos nt + \sin n\theta_0 \sin nt] \quad (20)$$

where the axial variation outside the end-roll region (near $z = 1$) is captured in $a_n(z)$ and where θ has been replaced by $t+\theta_0$ (note, $a_n(z)$ is determined using the imposed flux distribution $q'(\theta, z)$). Based on this form of the flux boundary condition, the solution is given by

$$T' = \frac{1}{\sqrt{Pe}}\sum_{n=1}^{\infty} a_n(z) \times \left\{\frac{1}{\sqrt{n}} e^{-\sqrt{n/2}\eta} \sin\left[n(t+\theta_0)+\frac{\pi}{4}-\eta\sqrt{\frac{n}{2}}\right] - \frac{2}{\pi}\int_0^{\infty}\left(\frac{u^2\cos n\theta_0 + n\sin n\theta_0}{n^2+u^4}\right)e^{-u^2 t}\,dt\right\} \quad (21)$$

where the first term on the right is the steady-state solution obtained by setting $T'_{,t} = 0$ in (10).

The behavior of this solution over long time periods can be determined using Laplace's method. Substituting $\theta - \theta_0 = t$, we find that as the steady-state is approached, the transient part of the solution decays as $t^{-1/2}$:

$$T' = \frac{1}{\sqrt{Pe}}\sum_{n=1}^{\infty} a_n(z)\left\{\frac{1}{\sqrt{n}} e^{-\sqrt{n/2}\eta}\sin\left[n\theta+\frac{\pi}{4}-\eta\sqrt{\frac{n}{2}}\right] - \frac{1}{n\sqrt{\pi t}}\sin[n(\theta-t)]+,\cdots,\right\}. \quad (22)$$

Thus, boundary layer transients die out somewhat slowly. For example, at a typical rotation rate of ~ 20 rad s^{-1}, 5 s (12 revolutions) must elapse for every order of magnitude reduction in the time-dependent term. We note that the experimental transients reported in [11] appear to decay like $t^{-1/2}$. However, the reported data is insufficient to allow a rigorous test.

In closing this section, we mention Yuen's work [2] which showed that accurate temperature calculations based on Fourier expansions require inclusion of a large number of modes. This feature arises due to typically large circumferential heat flux variations. Although Fourier solutions like that in (21) prove numerically inefficient, they are convenient for examining qualitative boundary layer behavior.

Steady-state boundary layer

Considering steady boundary layer behavior, we avoid the computational difficulties associated with Fourier solutions by expressing the solution to (17) as a Duhamel integral [16]:

$$T' = -\frac{1}{\sqrt{Pe\pi}}\int_0^{\theta-\theta_0} \tau^{-1/2} q'(\theta-\theta_0-\tau, a) \times \exp(-\eta^2/4\tau)\,d\tau. \quad (23)$$

In order to test this solution, we impose a surface heat flux distribution which was recently reconstructed by Huang *et al.* via an inverse approach [10] (see Model Illustration III). The flux distribution is shown in Fig. 2(a) and was estimated at 10° increments, based on the experimental temperature measurements reproduced in Fig. 2(c). The integral in (23) is evaluated using Gaussian quadrature and assumes linear variations between each of the 36 estimated fluxes.

Figure 2(b) compares calculated and experimental temperature measurements on the roll surface, while Fig. 2(c) compares calculated and measured temperatures at a depth 0.2 mm below the surface. As shown, calculated temperature distributions are in reasonable agreement with experimental measurements at both locations. The level of agreement suggests the validity of the asymptotic model and the relative accuracy of estimated flux distribution in Ref. [10].

MODEL ILLUSTRATION II: CORE HEAT TRANSFER DUE TO TIME- AND SPACE-DEPENDENT SURFACE HEAT FLUX DISTRIBUTIONS

Core heat transfer is described by eqns (15)–(16d). Although a number of particular problems can be considered [9, 19], we will assume that the strip width is fixed and is less than the roll width. Under arbitrary surface heating (and/or cooling) conditions, where $\bar{q} = \bar{q}(z, \bar{t})$, an integral solution can be obtained using a Green's function:

$$\bar{T}(r, z, t) = \int_0^t \left[\int_0^{1/A} \bar{q}(\bar{z}', \tau) G(r, \bar{z}, t|r' = 1, \bar{z}', \tau) 2\pi\, d\bar{z}'\right] d\tau. \quad (24)$$

Here, the two-dimensional Green's function, G, is the product of two one-dimensional Green's functions, G_{R02} and G_{Z22}, where [20]:

$$G_{R02}(r, t|r', \tau) = \frac{1}{\pi} + \frac{1}{\pi}\sum_{n=1}^{\infty} \exp[\beta_n^2(t-\tau)]\frac{J_0(\beta_n r)J_0(\beta_n r')}{J_0^2(\beta_n)} \quad (24a)$$

and

$$G_{Z22}(z, t|z', \tau) = 1 + 2\sum_{n=1}^{\infty} \times \exp[\gamma_n(t-\tau)]\cos(\gamma_n z)\cos(\gamma_n z') \quad (24b)$$

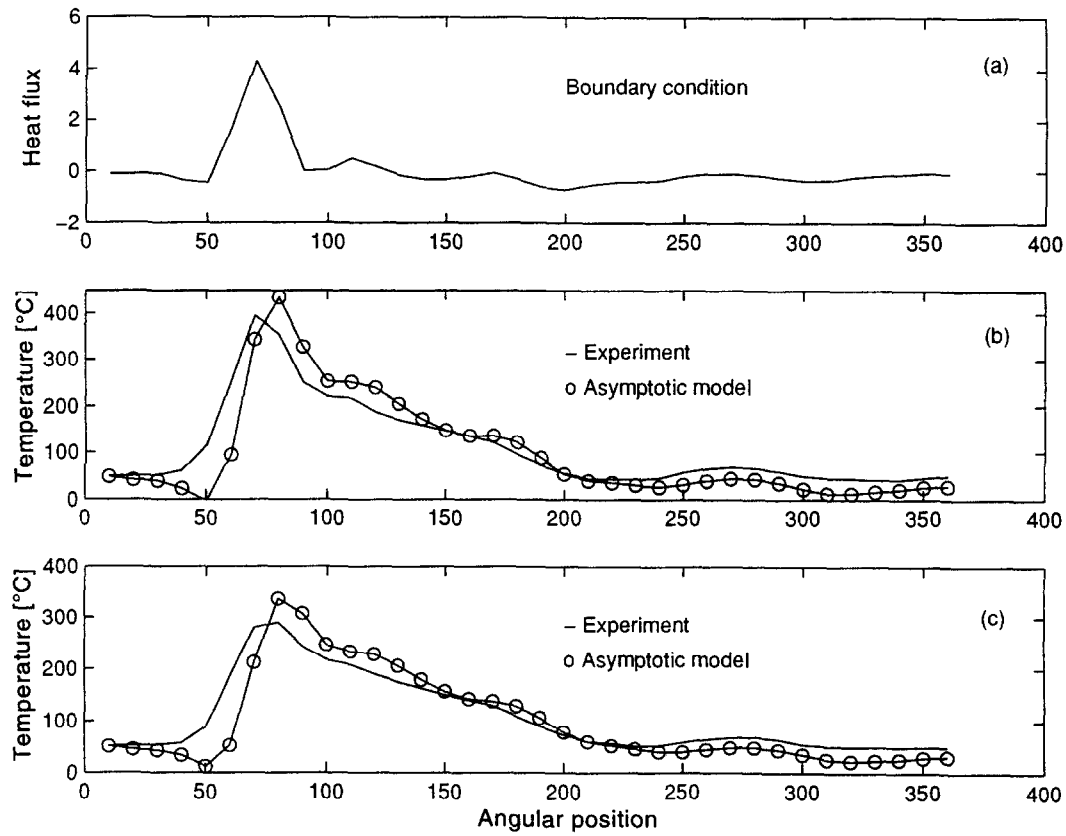

Fig. 2. Comparison between calculated temperatures and experimental temperatures reported in Ref. [10]: (a) the reconstructed surface heat flux distribution [10] used in eqn (23). The heat flux is plotted in units of 10^7 W m^{-2}; (b) measured and calculated roll surface temperatures; (c) measured and calculated temperatures at a depth 0.2 mm below the roll surface.

and where the eigenvalues β_n in (24a) are the roots of $J_1(\beta) = 0$ and $\gamma_n = n\pi$ in (24b).

To gain insight into this solution, let $\tilde{q} = q_0 = $ constant, a condition that is nominally approached, e.g. during the latter stages of the hot soaking operation [13]. Integration of (24) then yields

$$\bar{T} = q_0\left[2\tilde{t}+2\sum_{n=1}^{\infty}\frac{1}{\beta_n^2}\frac{J_0(\beta_n r)}{J_0(\beta_n)} -2\sum_{n=1}^{\infty}\frac{\exp(-\beta_n^2 t)}{\beta_n^2}\frac{J_0(\beta_n r)}{J_0(\beta_n)}\right]. \quad (25a)$$

This solution can be verified by first noting that when $\tilde{q}$ is constant, the problem becomes one-dimensional in r. Using the Laplace transform on the corresponding 1-D form of (15), we obtain [16]

$$\bar{T} = q_0\left[2\tilde{t}+\frac{r^2}{2}-\frac{1}{4}-2\sum_{n=1}^{\infty}\frac{\exp(-\beta_n^2\tilde{t})}{\beta_n^2}\frac{J_0(\beta_n r)}{J_0(\beta_n)}\right]. \quad (25b)$$

Since $\bar{T}(r, \tilde{t} = 0) = 0$, eqn (25b) shows that

$$\frac{r^2}{2}-\frac{1}{4} = 2\sum_{n=1}^{\infty}\frac{1}{\beta_n^2}\frac{J_0(\beta_n r)}{J_0(\beta_n)}$$

and, therefore, also shows the equivalence of eqns (25a) and (25b). Physically, the solution [eqn (25a) or (25b)] indicates that after a relatively short time lag ($\tilde{t} > \sim\beta_1^{-2} \sim 0.08$), the core temperature increases approximately linearly with time. As expected, the maximum and minimum temperatures occur at the surface and axis of rotation, respectively.

MODEL ILLUSTRATION III: INVERSE ESTIMATION OF BOUNDARY FLUX DISTRIBUTION

In the last illustration, we estimate the azimuthal heat flux distribution on a work roll using data reported by Huang *et al.* [10]. These investigators developed an inverse procedure for estimating the flux distribution based on a finite difference direct solver and conjugate gradient minimization. In the present illustration, direct solutions are obtained using the Duhamel solution given by eqn (23) while a whole domain method [17] comprises the inverse scheme.

Based on data in [10], we assume that the flux dis-

tribution is invariant on the fast time scale. The distribution is then parameterized using:

$$\mathbf{q} = (q_1, q_2, \ldots, q_N) \tag{26}$$

where $q_j = q(\theta = \pi \cdot j/18)$ and $N = 36$. A least squares function $S(\mathbf{q})$ is minimized in order to arrive at an estimate for $\mathbf{q}$, where

$$S(\mathbf{q}) = \sum_{j=1}^{N} (Y_j - T_j)^2. \tag{27}$$

Here, Y_j is the dimensionless measured surface temperature at position $\theta = \pi \cdot j/18$ and $T_j = T_j(\mathbf{q})$ is the corresponding calculated temperature. For any given $\mathbf{q}$, a continuous flux distribution is approximated using cubic splines, based on the 36 equally spaced flux magnitudes in $\mathbf{q}$. The 36 integrals represented by eqn (23) (one for each location θ_j) are calculated using Gaussian quadrature, while $S(\mathbf{q})$ is minimized using the multidimensional simplex minimization procedure [18]. In order to obtain a suitable sampling of the parameter space, the initial $N+1$ vertices $(\mathbf{q}_1^{(0)}, \mathbf{q}_2^{(0)}, \ldots, \mathbf{q}_{N+1}^{(0)})$ are generated randomly:

$$q_{i,j}^{(0)} = \lambda(1 - 2\kappa_j) \quad i = 1, \ldots, N+1, \quad j = 1, \ldots, N \tag{28}$$

where $q_{i,j}^{(0)}$ is the jth component of the ith initial parameter vector, λ is an amplification factor arbitrarily set equal to 4.0, and κ_j is a uniform random deviate between 0 and 1. (Note that final estimates are essentially independent of λ over $0.25 \leqslant \lambda \leqslant 5$.)

The property and parameter values used in the inverse solution are identical to those used in [10]: $\hat{\rho}_0 = 7830$ kg m^{-3}, $\hat{k}_0 = 48.1$ W m^{-1} K^{-1}, $\hat{c}_{p0} = 490$ J m^{-1} K^{-1}, $\hat{\Omega} = 155.6$ rpm, and $\hat{R} = 0.355$ m. We arbitrarily set $\hat{q}_s = 10^7$ W m^{-2} which fixes $\Delta\hat{T}_s$ at 182.2°C. (Note, $\hat{q}_s$ can be fixed at *any* magnitude since it cancels out the problem through the defining relationship for $\Delta\hat{T}_s$.) Finally, based on the temperature profiles reported in [10], we set $\hat{T}_i = 50$°C.

Inverse estimation results

In the following, we refer to the asymptotic-whole domain inverse technique as the AWD method and to the finite difference-conjugate gradient scheme in [10] as the FDC method. Experimental temperatures $\mathbf{Y}$ used in eqn (27) were measured at a depth 0.2 mm below the roll surface [10] and are reproduced in Fig. 3(c). Corresponding surface heat flux distributions, estimated by both AWD and FDC, are shown in Fig. 3(a). In addition, estimated temperature distributions on the roll surface and at the measurement depth, each obtained by the AWD method, are compared against corresponding experimental temperature distributions in Figs 3(b, c), respectively.

Referring to Fig. 3(a), it is apparent that the AWD-

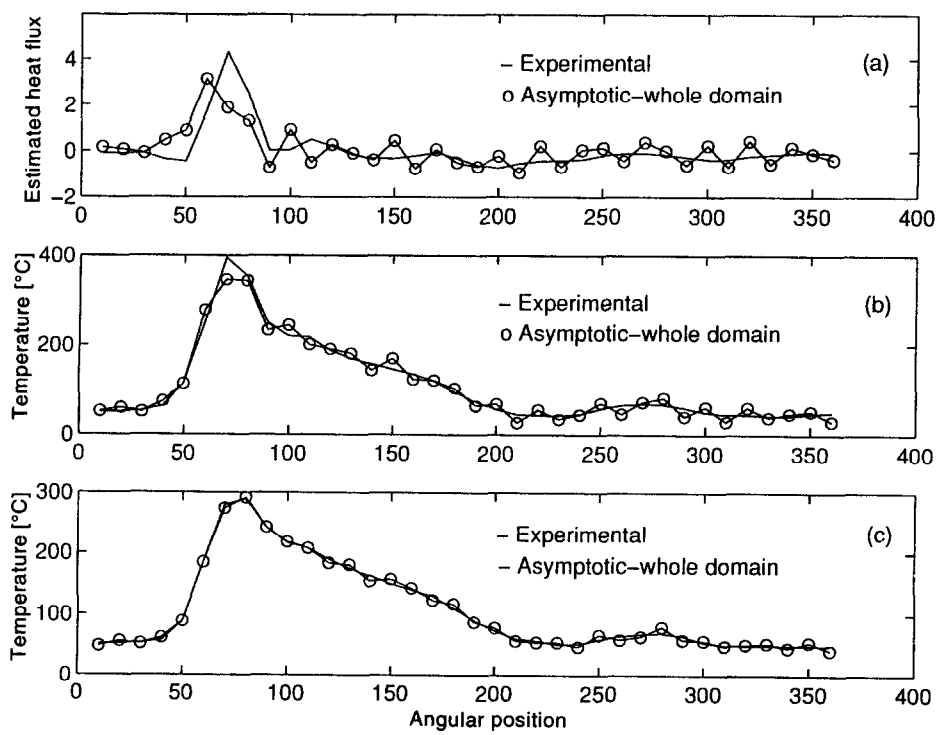

Fig. 3. Estimated heat flux and temperature distributions: (a) estimated surface heat flux distributions obtained by the method in Ref. [10] (solid line) and by the asymptotic-whole domain method (AWD) (circles). The heat flux is plotted in units of 10^7 W m^{-2}; (b) measured and AWD-estimated surface temperature distributions; (c) measured and AWD-estimated temperatures at a depth 0.2 mm below roll surface.

based flux estimate is qualitatively and quantitatively consistent with the FDC-based estimate. Note that the high flux region near $\theta \sim 75°$ corresponds to the roll bite. Also note that while both flux estimates are based on linear direct models, the relatively large temperature variation suggests that nonlinear direct models, represented for example by eqn (10), would provide more accurate estimates. Although the AWD estimate is somewhat more oscillatory than the FDC estimate, the oscillations can presumably be minimized by regularizing the inverse solution [10, 13, 17, 18], by increasing the ratio of measurements to the number of parameters describing **q** (here equal to 1), or by coupling the asymptotic direct model to a more sophisticated minimization scheme. The degree of mismatch between the two estimates might be similarly reduced by one or more of these approaches. [Note, regularization was not performed since the error S in (27) did not reduce to sufficient levels (S must approach $N\sigma^2$ where σ is the characteristic measurement error). This may be an artifact of the simplex minimization procedure, which tends to "float" near minimum points.] With respect to strip rolling, the relative simplicity of the AWD approach makes it an attractive alternative to potential finite difference and finite element-based inverse methods.

The level of agreement between estimated and experimental surface temperatures in Fig. 3(b) is comparable to that obtained by Huang *et al.* (by the FDC approach) [10]. It should be noted, however, that the FDC estimate of peak temperature is approximately 6% more accurate than the corresponding AWD-based estimate. Good agreement between estimated and measured temperatures is observed at the measurement site in Fig. 3(c). It should be kept in mind, however, that this result largely reflects adequacy of the minimization algorithm and is essentially independent of the model used for direct calculations. Note, oscillatory flux estimates originally observed near $\theta \sim 0 \sim 2\pi$ were displaced to $\theta_f = 25/12\pi$ by continuing the inverse calculation to θ_f. This procedure, introduced by Huang *et al.* [10], improves the level of agreement between measured and estimated surface temperatures, and thus presumably improves the accuracy of the flux estimate.

CONCLUSIONS

An asymptotic model of work roll heat transfer has been developed. The model provides a unified framework for relating prior roll heat transfer models and provides a convenient basis for future formulations. The model is illustrated three ways. First, we examine the behavior of the near surface thermal boundary layer under steady and dynamic conditions. It is found that the unsteady boundary layer relaxes to the cyclic steady state at a rate proportional to $t^{1/2}$, where $t = \hat{t}\hat{\Omega}$. Under steady conditions and subject to a reconstructed surface heat flux distribution, the model predicts temperature distributions which are in reasonable agreement with previously reported measurements. In the second illustration, we determine core heating (or cooling) produced by an arbitrary (circumferentially averaged) surface heat flux distribution. Insight into the resulting integral solution is obtained by examining an idealized case of constant flux heating. Following a short time-lag, it is found that the corresponding core temperature increases linearly with time. In the last illustration, the circumferential heat flux distribution on a work roll is estimated by an inverse procedure. It is found that the asymptotic-whole domain inverse approach provides relatively accurate temperature estimates, while flux estimates are quantitatively and qualitatively similar to those obtained by a recently developed finite difference-conjugate gradient inverse method [10].

Acknowledgements—This work was supported by the National Science Foundation (R.E.J.) and by an Alcoa Foundation Science Support Grant (R.G.K.).

REFERENCES

1. Peck, C. F., Bonetti, J. M. and Mavis, F. T., Temperature stresses in iron work rolls. *Iron Steel Engineering Year Book*, 1954, p. 389.
2. Yuen, W. Y. D., On the steady-state temperature distribution in a rotating cylinder subject to heating and cooling over its surface. *Journal of Heat Transfer*, 1984, **106**, 578–585.
3. Patula, E. J., Steady-state temperature distribution in a rotating roll subject to surface fluxes and convective cooling. *Journal of Heat Transfer*, 1981, **103**, 36–41.
4. Tseng, A. A., A numerical heat transfer analysis of strip rolling. *Journal of Heat Transfer*, 1984, **106**, 512–517.
5. Yuen, W. Y. D., On the heat transfer of a moving composite strip compressed by two rotating cylinders. *Journal of Heat Transfer*, 1985, **107**, 541–548.
6. Tseng, A. A., Tong, S. X., Maslen, S. H. and Mills, J. J., Thermal behavior of aluminum rolling. *Journal of Heat Transfer*, 1990, **112**, 301–308.
7. Yuen, W. Y. D., Temperature fields in sliding solids with internal heat sources. *International Journal of Heat and Mass Transfer*, 1993, **36**, 3711–3722.
8. Yuen, W. Y. D., The thermal boundary layer in a rotating cylinder subject to prescribed surface heat fluxes. *International Journal of Heat and Mass Transfer*, 1994, **37**, 605–618.
9. Guo, R.-M., Two-dimensional transient thermal behavior of work rolls in rolling process. In *Recent Advances in Heat Transfer and Micro-Structure Modelling for Metal Processing*, MD-Vol. 67, ed. R.-M. Guao and J. J. M. Too. ASME, New York, 1995, pp. 79–89.
10. Huang, C. H., Ju, T. M. and Tseng, A. A., The estimation of surface thermal behavior of the working roll in hot rolling process. *International Journal of Heat and Mass Transfer*, 1995, **38**, 1019–1031.
11. Tseng, A. A., Chang, J. G., Raudensky, M. and Horsky, J., An inverse finite element evaluation of roll cooling in hot rolling of steels. *Journal of Materials Processing and Manufacturing Science*, 1995, **3**, 387–408.
12. Macqueene, J. W., Akau, R. L., Krutz, G. W. and Schoenhals, R. J., Development of inverse finite element techniques for evaluation of measurements obtained from welding processes. *Proceedings of the Second National Symposium on Numerical Methods in Heat Transfer*, Hemisphere, Washington D.C., 1983, pp. 149–164.
13. Keanini, R. G., Inverse method for estimating time- and

space-dependent surface heat flux distributions during high speed rolling. *International Journal of Heat and Mass Transfer* (in press).
14. Schetz, J. A., *Boundary Layer Analysis*. Prentice-Hall, New York, 1993, pp. 93–114.
15. Tseng, A. A., A generalized finite difference scheme for convection-dominated metal-forming problems. *International Journal of Numerical Methods in Engineering*, 1984, **20**, 1885–1900.
16. Carslaw, H. S. and Jaeger, J. C., *Conduction of Heat in Solids*, 2nd edn. Oxford University Press, Oxford, 1959, p. 76.
17. Beck, J. V., Blackwell, B. and St Clair, C. R., *Inverse Heat Conduction*. Wiley, New York, 1985, pp. 134–144.
18. Press, W. H., Flannery, B. P., Teukolsky, S. A. and Vetterling, W. T., *Numerical Recipes*, 2nd edn. Cambridge University Press, New York, 1992, p. 802.
19. Robinson, N. I. and de Hoog, F. R., Angularly averaged heat transfer for a roller used in strip rolling. *Mathematical Engineering in Industry*, 1996, **5**, 281–304.
20. Beck, J. V., Cole, K. D., Haji-Sheikh, A. and Litkouhi, B., *Heat Conduction Using Green's Functions*. Hemisphere, London, 1992, p. 103.